International Journal of Thermal Sciences 100 (2016) 391–400

Contents lists available at ScienceDirect

International Journal of Thermal Sciences

journal homepage: www.elsevier.com/locate/ijts

General semi-empirical correlation for condensation of vapor on tubes at different orientations

S.A. Nada [a, *], H.M.S. Hussein [b]

[a] Department of Mechanical Engineering, Benha Faculty of Engineering, Benha University, Benha, 13511 Qalyubia, Egypt
[b] Solar Energy Department, National Research Centre, El-Behooth Street, Dokki, 12622 Giza, Egypt

ARTICLE INFO

Article history:
Received 14 June 2015
Received in revised form
6 October 2015
Accepted 6 October 2015
Available online xxx

Keywords:
Film wise condensation
Outside tubes
Effect of tube inclination
Theoretical
Experimental
Semi-empirical correlation

ABSTRACT

Analytical and experimental investigations for condensation of saturated vapor on smooth tube at different orientations are presented. An analytical model was developed starting from mass, momentum and energy equations. The model was solved analytically by the method of characteristics with the aid of a computer program. In the experimental work, heat transfer due to film wise condensation of saturated steam on smooth tube has been investigated for different tube inclinations. Seven series of experiments were conducted at tube inclination angles of 0°, 10°, 20°, 30°, 45°, 60° and 90° with the vertical. Variation of Nusselt number with temperature difference and inclination angles are investigated from the theoretical and experimental results. Both experimental and theoretical results showed the increase of the Nusselt number with the decrease of the temperature difference and the increase of the tube inclination angle from the vertical. Comparison between the experimental and theoretical results showed fair agreement for vertical and horizontal tubes. However, the deviation increased with tilting the tube from horizontal or vertical position. General semi-analytical correlation was deduced from the experimental and theoretical results to fairly predict the Nusselt number for any tube inclination.

© 2015 Elsevier Masson SAS. All rights reserved.

1. Introduction

Tube-side condensation is used in a wide range of engineering applications such as refrigeration, air conditioning, space heating, food industry, automotive and process industries. Nowadays, higher energy efficiency and economic incentive requirements and material saving considerations have increased the need for highly efficient heat transfer surfaces. Heat transfer in tube condensation strongly depends on surface orientation and the enhancement of condensate drainage rate.

Literature review revealed that studies of condensation on vertical and inclined tubes are very limited. In contrast, numerous theoretical and experimental studies were carried out on condensation inside horizontal, vertical and inclined tubes. Many theoretical studies [1–9] were conducted to find the condensate film thickness and condensation heat transfer coefficient at any point in the tube surface in terms of the orientation of the surface and tube surface temperature. The analysis was performed under the same assumptions of Nusselt's classical theory of film condensation [1]. At the same time, numerous experimental studies were carried out to verify theoretical analysis and obtaining experimental correlations to avoid error in the theoretical analysis due to Nusselt's assumptions. Hassan and Jakob [2] compared their analytical results with the experimental results for the condensation heat transfer coefficient on inclined cylinder. The experimental results were found to be 28–100% higher than the analytical results. They attributed this deviation due to the rippling of the condensate film that was not taken into account in the theoretical study.

Hussein et al. [3,4] presented theoretical and experimental analysis for wickless heat pipes of different cross section geometries and deduced a correlation for laminar-film condensation heat transfer coefficient in the condenser section of inclined wickless heat pipes flat-plate solar collector. The comparison between theoretical relation and experimental results by other investigators showed a good agreement. Wang and Ma [5] carried out theoretical and experimental studies on condensation inside vertical and inclined thermosyphons tube. They pointed out that no final conclusion can be drawn on the optimum inclination angle at which the maximum heat transfer coefficient can occur. They presented semi-empirical correlations for reflux condensation inside inclined and vertical tubes. Fiedler and Auracher [6] experimentally investigated heat transfer during reflux condensation of

* Corresponding author. Tel.: +20 1066611381 (mobile).
E-mail address: samehnadar@yahoo.com (S.A. Nada).

http://dx.doi.org/10.1016/j.ijthermalsci.2015.10.023
1290-0729/© 2015 Elsevier Masson SAS. All rights reserved.

Nomenclature

C_p	specific heat of cooling water, kJ/(kg K)
D	tube outside diameter, m
$d\dot{m}$	mass of element, kg
h	average heat transfer coefficient, W/(m^2 K)
h_{fg}	latent heat of vaporization, kJ/(kg K)
k	thermal conductivity of liquid film, W/(m K)
L	tube length, m
$\dot{m}$	mass flow rate, kg/s
Nu	average Nusselt number, dimensionless
q	heat transfer rate, W
R	tube inner radius, m
r	radial distance measured from tube outer surface, m
Re	Reynolds number, dimensionless
T	temperature, °C

Subscripts

c	condensate
cw	cooling water
L	liquid
i	inlet
o	outlet
x	x-direction
ϕ	ϕ-direction
s	saturated steam
v	vapor
w	tube wall

Greek symbol

β	tube inclination angle with reference to the vertical, °
δ	film thickness, m
μ	dynamic viscosity, kg/m s
ρ	density, kg/m^3
ϕ	perimeter angle of the tube, °
ΔT	temperature difference between condensing steam and tube surface, °C

refrigerant R134a in an inclined small diameter tube. They found that the inclination angle has a significant effect on the heat transfer coefficient. Shah [7] presented general modified correlations for condensation inside vertical, inclined and horizontal tubes which can be applied for a wide range of fluid and geometric parameters. Meyer et al. [8] conducted experimental investigation on the effects of the saturation temperature and inclination angle on condensation of R134a flowing inside inclined tubes. The results showed (i) the increase of the heat transfer with the decrease of saturation temperature, and (ii) the existence of optimum inclination angle at which heat transfer is maximum. Wang and Du [9] presented a theoretical study for laminar film-wise condensation inside small diameters tubes. Lips and Meyer [10] reviewed condensation two phase flow inside horizontal and inclined tubes. The review showed that the inclination angle strongly affects the flow regime and the heat transfer.

Recently, a lot of theoretical and experimental works were conducted to study the effects of the presence of non-condensable gases on the condensation inside vertical, inclined and horizontal tubes [11,12]. Experimental correlations were presented to show the effect of the presence of non-condensable gases on the condensation rate. The studies showed that the presence of non-condensable gases adversely affect the condensation efficiency and heat transfer.

Condensation inside vertical and inclined tubes in case of upward vapor flow (Reflux condensation) is limited by flooding phenomenon where at a certain upward vapor velocity part of the condensate will be carried upward by the vapor and the other part is draining downward. Nada et al. [13,14] and English et al. [15] proposed correlations that are widely used in industry to predict the flooding point. Fiedler and Auracher [6] and Fiedler et al. [16] showed experimentally that the flooding point during reflux condensation in small diameter tubes is affected by the inclination angle. They showed that the optimum inclination angle at which the highest flooding vapor velocity can be reached is between 45° and 60°.

In spite of the several theoretical and experimental works and correlations for condensation inside horizontal, vertical and inclined tubes, the results of these works and correlations cannot be applied for condensation outside tubes where the phenomena and condensate film motion and drainage mechanism are totally different. Some theoretical and experimental studies have been reported on condensation heat transfer performance on vertical and horizontal tubes. However, a relatively small number of studies have been published on the performance of inclined tubes, where the flow of condensate film becomes two dimensional flow. Thomas [17] studied the effect of the presence of longitudinal rectangular fins on condensation heat transfer of saturated steam outside the tube. The study showed an increase of the heat transfer due to the presence of such fins. It was found that the film condensation enhancement coefficient increases with the decrease of heat flux and the increase of the number of fins. Domingo and Michel [18] studied condensation of Ammonia on smooth tube at various tilt angle. The results showed that the heat transfer coefficient increases as the tilt angle decreases from the vertical to horizontal position. Amin [19] presented an experimental investigation of heat transfer augmentation during condensation on vertical tubes using drainage caps. Experimental results showed that using drainage caps dramatically improve heat transfer rates.

In the present paper, comprehensive theoretical and experimental investigations of saturated vapor condensing outside tube at different orientations (vertical, horizontal and inclined at different angles of inclination) are presented. The effects of temperature difference, tube inclination angle and tube geometrical parameters are studied. Comparisons between theoretical and experimental results are quantified and investigated. General semi-empirical correlation is suggested for accurate estimation of Nusselt number during condensation on tubes at different orientations.

2. Theoretical analysis

To simplify the mathematical model, some assumptions are considered during the present theoretical analysis. The assumptions are the same of Nusselt [1] assumptions for condensation on vertical surface taking in consideration the effect of the buoyancy force. These assumptions are summarized as follows:

- The flow of the condensate film is laminar, uniform and steady.
- The vapor is considered dry, saturated, pure and free from non-condensable gases.
- The vapor velocity is very small, thus the shear stress at the vapor–liquid interface can be neglected.

- Convection heat transfer between the condensate film and the adjacent vapor is neglected and the heat transfer across the condensate film is by conduction.
- The tube surface temperature is uniform.
- The inertia force of the condensate film is neglected and the only force acting on the condensate film is the gravity force.
- Variation of the physical properties of the condensate film and the vapor are neglected.
- The condensate film thickness is negligible with respect to the tube radius.

2.1. Description of condensate motion

The expected path of the condensate film motion on inclined tube is shown in Fig. 1 where the droplet of the condensate film tends to move vertically downwards under the action of gravity, and at the same time the motion is constrained to be in contact with the tube surface. The expected distribution of the condensate film thickness around the surface of the inclined tube is illustrated in Fig. 1. The flow of the condensate film is two dimensional, in the axial and tangential direction, and symmetrical about the plan $\phi = 0$. The condensate film thickness is maximum at $\phi = \pi$ and minimum at $\phi = 0$ and increases as the axial distance measured from the top edge of the tube increases.

2.2. Mass conservation

Fig. 2a shows an element of the condensate film on the tube surface. The element is taken at a radial distance r from the tube surface and ends at the liquid–vapor interface. The mass flow rates of the condensate entering and exit the element in the axial and tangential directions are given by:

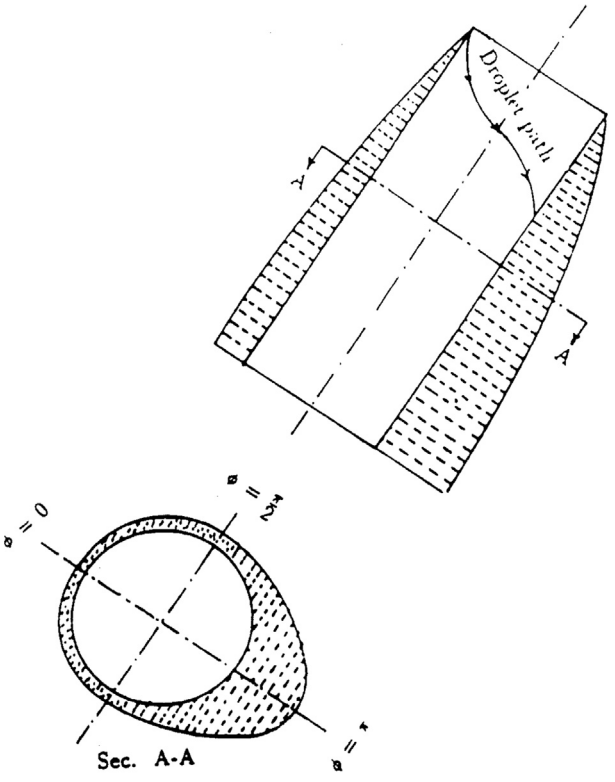

Fig. 1. Condensate film motion and thickness distribution on inclined tube.

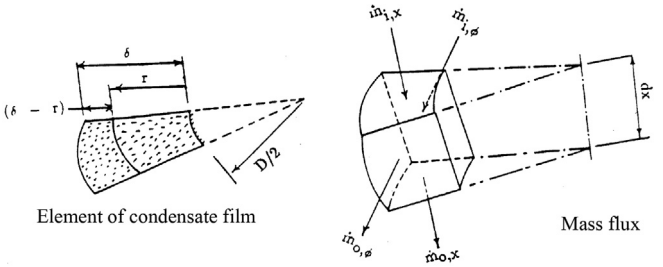

a- Element of condensate film and mass

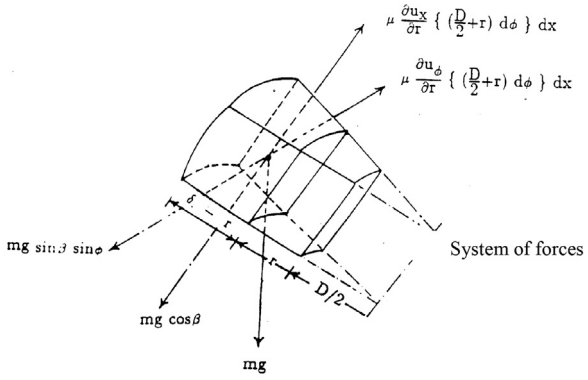

b- System of forces

Fig. 2. Element of the condensate film on tube surface and system of forces acting on it.

$$\dot{m}_{i,x} = \rho_L \int_0^{\delta} u_x (D/2 + r)\mathrm{d}\phi\mathrm{d}r \tag{1}$$

$$\dot{m}_{o,x} = \dot{m}_{i\cdot x} + \frac{\partial}{\partial x}(\dot{m}_{i\cdot x})\mathrm{d}x \tag{2}$$

$$\dot{m}_{i,\phi} = \rho_L \int_0^{\delta} u_\phi \,\mathrm{d}x\mathrm{d}r \tag{3}$$

$$\dot{m}_{o,\phi} = \dot{m}_{i\cdot\phi} + \frac{\partial}{\partial \phi}(\dot{m}_{i\cdot\phi})\mathrm{d}\phi \tag{4}$$

The net increase in the condensate mass flow rate is

$$d\dot{m} = (\dot{m}_{o\cdot x} - \dot{m}_{i\cdot x}) + (\dot{m}_{o\cdot\phi} - \dot{m}_{i\cdot\phi}) \tag{5}$$

Combining Eqns. (1)–(5) and neglecting the condensate film thickness with respect to the tube diameter, it is found that

$$d\dot{m} = \rho_L \left(\frac{\partial}{\partial x} \int_0^{\delta} \frac{D}{2} u_x \,\mathrm{d}r\mathrm{d}\phi\mathrm{d}x + \frac{\partial}{\partial \phi} \int_0^{\delta} u_\phi \,\mathrm{d}r\mathrm{d}\phi\mathrm{d}x \right) \tag{6}$$

2.3. Momentum equation

Fig. 2b shows the system of forces acting on the condensate film element. The element is acted by the force of gravity downwards, the buoyancy force upwards and the viscous force components in the axial and tangential directions. As the element is in equilibrium under this system of forces, balances of forces in the tangential and axial directions can be represented by the following equations:

$$mg \sin\beta \sin\phi = \mu \frac{\partial u_\phi}{\partial r}(D/2 + r)\mathrm{d}\phi\mathrm{d}x \tag{7}$$

$$mg \cos\beta = \mu \frac{\partial u_x}{\partial r}(D/2 + r)\mathrm{d}\phi\mathrm{d}x \tag{8}$$

where m = mass of the element − mass of the displaced vapor

$$m = (\rho_L - \rho_v)(D/2 + r)\mathrm{d}\phi(\delta - r)\mathrm{d}x \tag{9}$$

Substituting Eqn. (9) in Eqns. (7) and (8) yields

$$\mu \frac{\partial u_x}{\partial r} = (\rho_L - \rho_v) g \cos\beta(\delta - r) \tag{10}$$

$$\mu \frac{\partial u_\phi}{\partial r} = (\rho_L - \rho_v) g \sin\beta \sin\phi(\delta - r) \tag{11}$$

Integrating Eqns. (10) and (11) under the boundary conditions $u_x = u_\phi = 0$ at $r = 0$ one can get

$$u_x = (\rho_L - \rho_v) g \cos\beta r(\delta - r/2)/\mu \tag{12}$$

$$u_\phi = (\rho_L - \rho_v) g \sin\beta \sin\phi r(\delta - r/2)/\mu \tag{13}$$

2.4. Energy equation

Applying energy balance on the studied element gives that the rate of heat released during vapor condensation is the same heat conducted across the thickness (δ) of the condensate film element [1], i.e.

$$\frac{k\Delta T}{\delta}(D/2)\mathrm{d}\phi\mathrm{d}x = d\dot{m}h_{fg} \tag{14}$$

Substituting Eqns. (12)–(14) into Eqn. (6), yields

$$\frac{k\Delta T}{\delta g h_{fg}} = \rho_L \left(\frac{2}{D}\frac{\partial}{\partial\phi}\int_0^\delta \frac{\rho_L - \rho_v}{\mu}\sin\beta \sin\phi\left(\delta r - r^2/2\right)\mathrm{d}r + \frac{\partial}{\partial x}\int_0^\delta \frac{\rho_L - \rho_v}{\mu}\cos\beta\left(\delta r - r^2/2\right)\mathrm{d}r \right) \tag{15}$$

Integrating the last Eqn. (15) and substituting by

$$Y = \frac{\delta^4 2 g h_{fg}(\rho_L - \rho_v)\sin\beta}{3Dk\mu\Delta T} \quad \text{and} \quad Z = \frac{2x}{D\cot\beta} \tag{16}$$

It can be found that

$$\frac{\partial Y}{\partial Z} + \sin\phi\frac{\partial Y}{\partial\phi} = \frac{4}{3}(1 - Y\cos\phi) \tag{17}$$

Eqn. (17) is a nonlinear first order partial differential equation and its solution gives the condensate film thickness at any point on the surface of the tube. The boundary conditions of this equation is that the condensate film thickness equals zero at the upper edge of the tube for any perimeter angle ϕ, i.e.

$$Y(Z, \phi) = 0 \text{ at } Z = 0 \text{ and } 0 \le \phi < 2\pi \tag{18}$$

Under the boundary condition given by Eqn. (18), Eqn. (17) can be solved analytically by the method of characteristics as described by Smith [20]. Smith showed that the partial differential equation in the form of Eqn. (17) can be obtained by investigating the possibility of finding a direction at each point of the integral surface $Y = f(Z, \phi)$ along which the partial differential equation is transformed to an ordinary differential equation. This direction is called the characteristics curve. Smith showed that the solution along this characteristics curve is given by

$$\mathrm{d}Z = \frac{\mathrm{d}\phi}{\sin\phi} = \frac{\mathrm{d}Y}{4/3(1 - Y\cos\phi)} \tag{19}$$

The equation of the characteristics curves is given by

$$\mathrm{d}Z = \frac{\mathrm{d}\phi}{\sin\phi} \tag{20}$$

Integrating Eqn. (20), gives

$$e^{-Z}\tan\frac{\phi}{2} = C_1 \tag{21}$$

The solution of Eqn. (19) along these characteristics curves is given by

$$\frac{\mathrm{d}\phi}{\sin\phi} = \frac{\mathrm{d}Y}{4/3(1 - Y\cos\phi)} \tag{22}$$

Hence,

$$\frac{\mathrm{d}Y}{\mathrm{d}\phi} + \frac{4}{3}\cot\phi Y = \frac{4}{3}\mathrm{cosec}\,\phi \tag{23}$$

Eqn. (23) is an ordinary linear first order differential equation. The solution of this equation has the following form as given by Wylie and Barret [21].

$$Y(Z, \phi) = e^{-\frac{4}{3}\int \cot\phi\,\mathrm{d}\phi}\left(\int \frac{4}{3}\left(e^{\frac{4}{3}\int \cot\phi\,\mathrm{d}\phi}\,\mathrm{cosec}\,\phi\,\mathrm{d}\phi \right) + C_2 \right) \tag{24}$$

Conducting the above integration and using the boundary condition $Y(0, \phi) = 0$, Eqns. (12) and (24) can be solved together to give

$$Y(Z,\phi) = \frac{4}{3}\sin\phi^{-4/3}\left(\int_0^\phi \sin\phi^{1/3}\mathrm{d}\phi - \int_0^{2\,arc\tan\left(e^{-Z}\tan\phi/2\right)} \sin\phi^{1/3}\mathrm{d}\phi \right) \tag{25}$$

By substituting Eqn. (16) into Eqn. (25), the condensate film thickness at any point on the tube surface can be expressed in the form

$$\delta(x, \phi) = \left(\frac{2Dk\mu\Delta T}{h_{fg}\rho_L(\rho_L - \rho_v)g\sin\beta} \right)^{1/4} \sin\phi^{-1/3}\left(\int_0^\phi \sin\phi^{1/3}\,\mathrm{d}\phi - \int_0^{2\,arc\,\tan\left(e^{-2x/D\,\tan\beta}\,\tan\phi/2\right)} \sin\phi^{1/3}\,\mathrm{d}\phi \right)^{1/4} \tag{26}$$

The local heat transfer coefficient at any point on the tube surface is given by

$$h(x,\phi) = \frac{k}{\delta(x,\phi)} \tag{27}$$

And the average heat transfer coefficient is given by

$$\overline{h} = \frac{k}{\pi L}\int_0^L \int_0^\pi \delta^{-1}(x,\phi)\mathrm{d}\phi\mathrm{d}x \tag{28}$$

Eqn. (28) gives the average heat transfer coefficient for each tube length and tube diameter in terms of the inclination of the tube with respect to the vertical and the temperature difference between the tube outer surface and the condensing vapor. Integration of Eqn. (26) cannot be obtained analytically, however it can be easily obtained numerically with the aid of a simple computer program.

Eqns. (26)–(28) obtained for vapor condensing outside an inclined tube can be considered as a general equation for vapor condensing on any surface orientations. Nusselt equations for vapor condensing on vertical tube, horizontal tube and inclined flat plat can be derived from Eqns. (26)–(28) by the substitution $\beta = 0$, $\beta = 90$ and $D = \infty$, respectively.

3. Experimental setup and procedure

3.1. Experimental setup

A schematic diagram of the experimental setup is shown in Fig. 3. The steam flows from the steam generator (1) to a steam super heater (2) through a steam valve (3) that regulates the steam flow rate. Superheated steam at 1 °C superheat leaves the super heater and enters the condenser (4). The steam condenses around the condenser tube. The cooling water required for the condenser comes from a constant head tank (5). The condensate exits the condenser via a steam trap (6) to a graduated vessel (7) to measure its mass flow rate. The steam generator is a vertical, electrically heated boiler. Nine electrical heaters, each 3 kW fitted at the lower cover of the steam generator are used to generate saturated steam. The steam generator is fitted with droplet water separator, thermometer, water indicator, pressure gauge, water inlet valve, drain valve and steam exit valve. An electric steam super heater with a power of 1.8 kW is used to eliminate any moisture content carried out with the steam leaving the boiler. The steam super heater rises the temperature of the steam by about 1 °C above the saturation temperature. The electric power of the steam super heater is controlled by an electric variac to maintain the 1 °C superheat.

The test section of the experimental setup is the condenser. The condenser is a shell and tube condenser. The condenser shell is made from a steel pipe of 330 mm outer diameter, 2 m length and 6 mm thickness. The test tube (condenser tube) is a stainless tube of 21 mm outer diameter and 1.5 mm thick fitted in the center of the condenser shell. To prevent water vapor from leaving the condenser with the condensate liquid, a steam trap is fitted with the condensate outlet.

The condenser shell is mounted on a mechanism fitted with a protractor to enable changing the inclination angle of the condenser between the vertical and horizontal position as required. To be able to vary the inclination angle, the test section is connected to the cooling water circuit and steam generator section by flexible pressure hoses. The condenser body is thermally insulated with 50 mm glass wall thermal insulation in order to reduce the heat losses from the condenser to the surrounding.

Fifteen K-type thermocouples are embedded on the outer tube at five axial locations, equally distributed along the length of the tube. Each axial location contains three thermocouples distributed at top, bottom and side around the circumference of the test section to be able to measure local wall temperatures (see Fig. 4). The thermocouples leads are embedded and soldered into 0.5 mm deep grooves and taken out through the annulus and fittings. Four other thermocouples are used to measure the cooling water temperature at inlet and exit to the test section and the steam temperatures at exit of steam generator and inlet of the condenser. All thermocouples are calibrated in a constant temperature bath and a measurement accuracy of ±0.15 °C are obtained. All the temperature signals were acquired using a data acquisition system and sent to a PC for data recording. Two letters graduated vessel is used to collect and measure the condensate during a long period of time, 1–2 min. A stop watch is used to estimate the time of the condensate collection. Accuracy of the eyesight during taking the measurements and unleakage of any condensate were assured. A water flow meter of 1% accuracy is used to measure the cooling water flow rate.

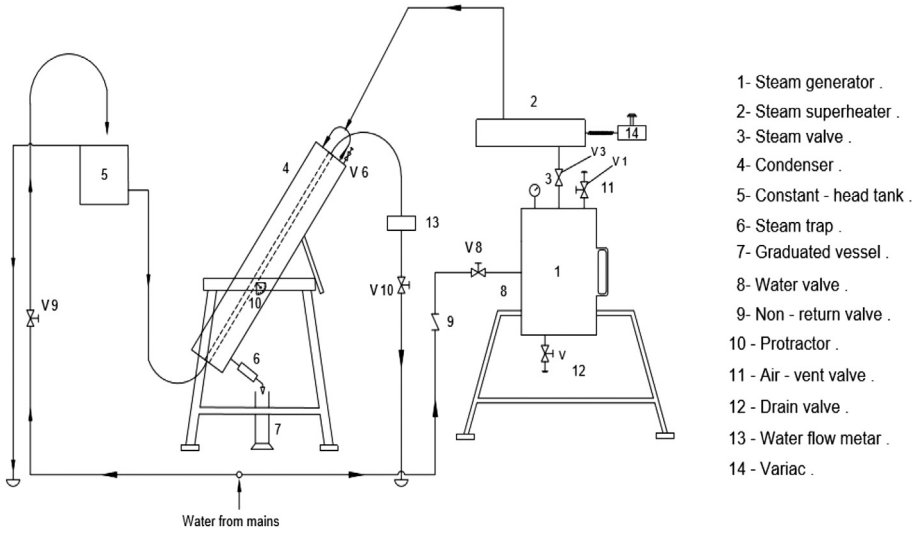

Fig. 3. Schematic diagram of the experimental setup.

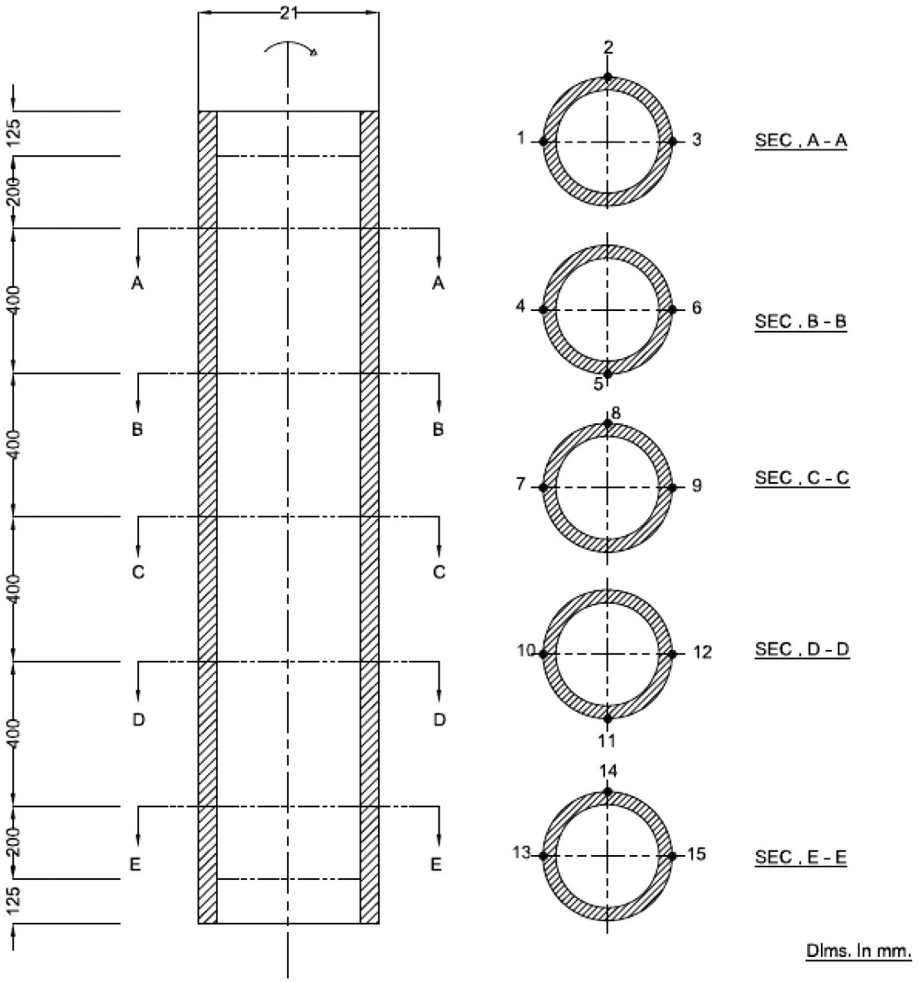

Fig. 4. Distribution of thermocouples on test section surface.

3.2. Data reduction

The heat released (q) from the vapor during its condensation on the test tube is estimated from the heat gained by the cooling water in the tube and is not calculated from the condensate flow rate. This is to avoid the effects of the of the heat losses from the condenser body and the error in estimating h_{fg} of the steam due to the small variation of steam pressure along test section, purity of water and amount of steam superheat and condensate water subcooled that may occur. Doing so, will reduce the error and uncertainty in estimating the heat transfer coefficient and the Nusselt number. The heat released (q) from the vapor during its condensation is calculated from:

$$q = \dot{m}_{cw} C_p (T_{cwo} - T_{cwi}) \tag{29}$$

To assure the reliability of the experiments, the heat (q_c) rejected from the vapor condensing on the test section and on the condenser shell (this part is expected to be very small due to the well thermal insulation of the condenser shell), is estimated from

$$q_c = \dot{m}_c h_{fg} \tag{30}$$

The heat transfer rates q and q_c were determined from both equations (29) and (30). The difference between the two heat flow rates was found to be within 4% for all the experiments and this confirms the reliability of the experiments.

The average condensation heat transfer coefficient on the test tube is calculated from

$$\overline{h} = \frac{q}{\pi D L (T_s - T_w)} \tag{31}$$

The average temperature at any thermocouples station along the tube length is [T(at $\phi = 0$) + T(at $\phi = \pi$) + T(at $\phi = \pi/2$) + T(at $\phi = 3\pi/2$)]/4. Since the condensate film thickness is symmetric around the plan passing by $\phi = 0$, $\phi = \pi$ (see Fig. 1), the condensate film thickness at $\phi = \pi/2$ equals to that at $\phi = 3\pi/2$ and this makes the temperature at $\phi = \pi/2$ equals to that at $\phi = 3\pi/2$. For this reason one thermocouple is placed either at $\phi = \pi/2$ or at $\phi = 3\pi/2$. In the first axial thermocouple station, the thermocouple is placed at $\phi = \pi/2$ and in the subsequent axial station it was placed at $\phi = 3\pi/2$ and so on. These changes between a thermocouple station and the next are to avoid any error that may come from the nonuniformity of the actual condensate film thickness. Therefore, the average temperature at any axial thermocouple station is calculated from [T(at $\phi = 0$) + T(at $\phi = \pi$) + 2T(at $\phi = \pi/2$)]/4 or [T(at $\phi = 0$) + T(at $\phi = \pi$) + 2T(at $\phi = 3\pi/2$)]/4. The overall average tube outer surface temperature is calculated by the arithmetic mean of the average temperature of the five thermocouples stations as follows (see Fig. 4).

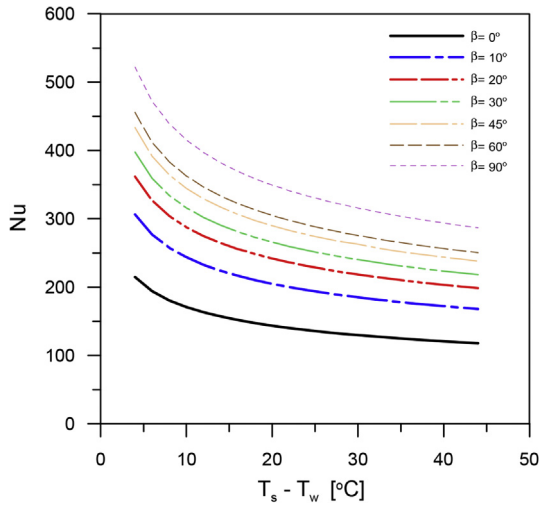

Fig. 5. Variation of theoretical Nusselt number at different inclination angles.

$$T_w = \frac{1}{20}(T_1 + 2T_2 + T_3 + T_4 + 2T_5 + T_6 + T_7 + 2T_8 + T_9 + T_{10} + 2T_{11} + T_{12} + T_{13} + 2T_{14} + T_{15}) \quad (32)$$

The average Nusselt number was normally calculated based on the tube length as the characteristics length of vertical tubes, while it was calculated based on the tube diameter as the characteristics length of horizontal tube. In this study and for the sake of comparisons, the Nusselt number is calculated based on the tube diameter for all tube orientations as given by:

$$Nu = \frac{\overline{h}D}{k} \quad (33)$$

Combining Eqns. (29) and (33) together, the expression of Nu can be put on the form

$$Nu = f(x_1, x_2, \ldots, x_n) \quad (34)$$

where x_1 to x_n are all the variables (temperatures, water flow rate, diameter) that affect the experimental determination of Nu. The uncertainty ΔNu in the value of Nu was estimated based on the procedure of Holman and Gajda [22] and is expressed as follows

$$\Delta Nu = \sqrt{\sum_{i=1}^{n}\left(\frac{\partial Nu}{\partial x_i}\Delta x_i\right)^2} \quad (35)$$

where Δx_i is the uncertainty in the x_i variable (temperatures, water flow rate, diameter). It was found that the uncertainty for all data of Nu ranges from 4 to 7 percent.

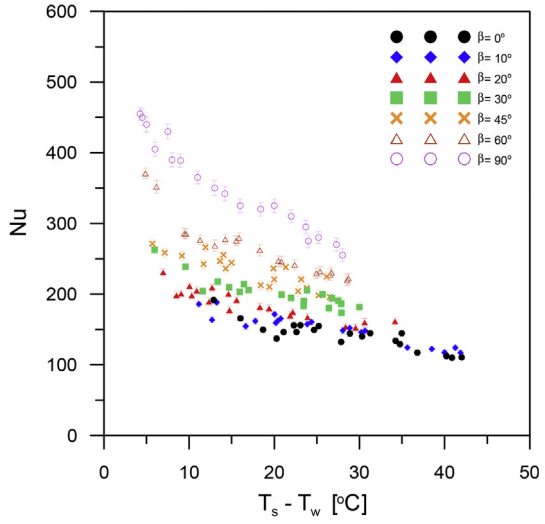

Fig. 6. Variation of experimental Nusselt number at different inclination angles.

4. Results and discussions

A simple computer program was developed to numerically evaluate the integrations in Eqns. (26)–(28). The program was run to estimate the Nusselt number for saturated steam condensing outside a tube having a diameter and length of 0.021 m and 2 m, respectively. The program was run for different tube inclination angles (β = 0, 10, 20, 30, 45, 60 and 90°) and different temperature differences between the tube outer surface and the saturated steam. Fig. 5 shows the variation of the obtained theoretical average Nusselt number with (T_s − T_w) at different tube inclinations. Moreover, the results obtained from the experimental data are shown in Fig. 6. Both theoretical and experimental results

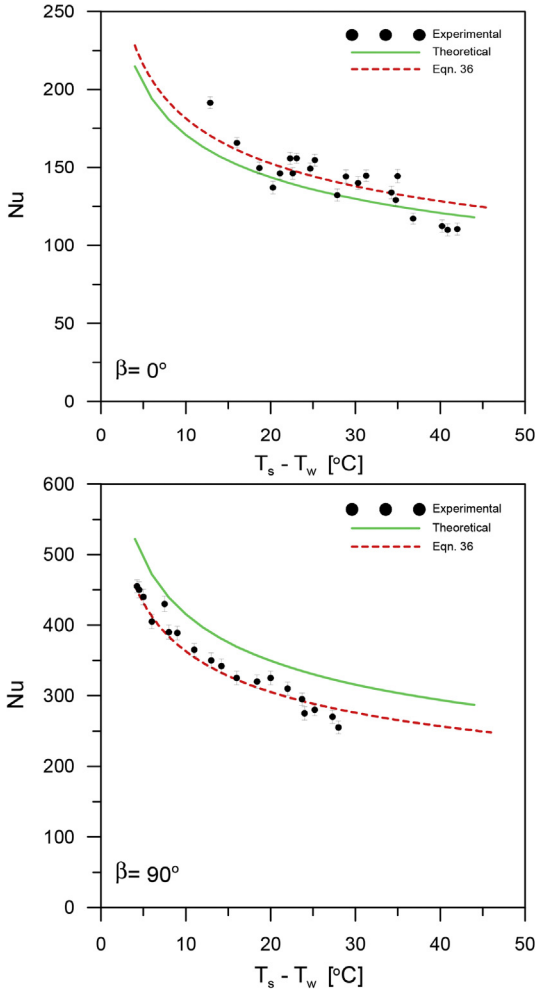

Fig. 7. Comparison between theoretical, semi-analytical and experimental Nusselt numbers for vertical and horizontal tubes (β = 0°, 90°).

show the increase of Nusselt number with the decrease of the temperature difference and the increase of the tube inclination from the vertical. The increase of the Nusselt number with the decrease of the temperature difference can be attributed to the decrease of the heat transfer rate with the decrease of the temperature difference. Decreasing the heat transfer rate decreases the rate of condensation and consequently decreases the condensate film thickness which decreases the thermal resistance and consequently increases the heat transfer coefficient and Nusselt number. This result agrees well with the previous theoretical and experimental results [1,5,6,8,9,19] for condensation of vapor around surfaces of different geometries and orientations where it was found that Nusselt number increases with the decease of the temperature difference.

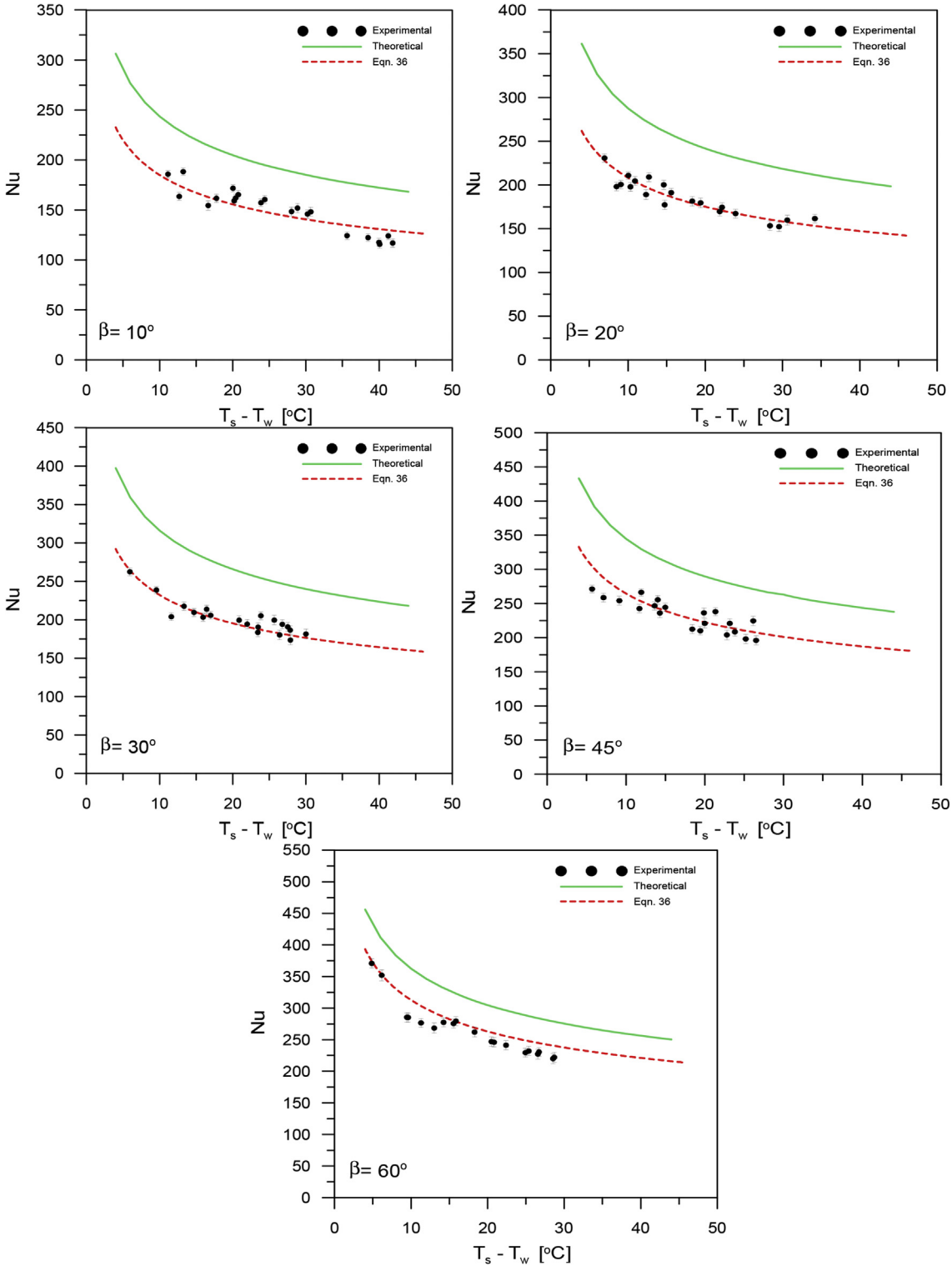

Fig. 8. Comparison between theoretical and experimental Nusselt numbers for inclined tubes.

The increase of the Nusselt number with increasing tube inclination from the vertical can be attributed to the behavior of condensate film motion and drainage on the surface of the tube and the path length of the condensate film on the surface of the tube until drainage. The length of the condensate film path until drainage depends on the tube inclination angle. As the tube inclination angle measured from the vertical increases, the path of the condensate film on the tube surface becomes shorter and the rate of condensate drainage increases reducing the amount of the condensate covering the tube surface and consequently decreases the thermal resistance and increases heat transfer coefficient. Fig. 5 reveals that the ratios between the Nusselt numbers of horizontal and vertical tubes obtained from theoretical work is 2.43 which equals to $(L/\pi D)^{1/4}$; i.e. the fourth root of the ratio between the condensate film path of the vertical and horizontal tubes. This ratio agrees with the ratio obtained by Nusselt [1]. However, Fig. 6 shows that the ratios between the Nusselt numbers of horizontal and vertical tubes for the different experimental data lie in the range 1.75–3. This deviation can be attributed to the simplified assumptions considered in driving the analytical equations and due to the uncertainty of the experimental work.

The comparison between analytical and experimental results is shown in Fig. 7 for vertical and horizontal tube and in Fig. 8 for inclined tubes. For vertical and horizontal tubes, Fig. 7 shows that the theoretical results can predict the experimental data with an error of about 10%. This small deviation can be attributed to the simplified assumptions considered in driving the analytical equations and due to the uncertainty of the experimental work. However, Fig. 8 shows that the deviation between the experimental and theoretical results increases with the increase of the inclination angle. This can be attributed to that the effect of the simplified assumptions in the analytical models starts to increase by inclining the tube from the vertical and the horizontal position. Moreover, the actual path of the condensate film motions and the condensate film drainage points may be different than the one considered in the analytical analysis. The theoretical model foresees drainage of the condensate when it reaches the angular position $\phi = \pi$ but in the actual path the drainage point is generally below this point, so that a thicker (average) condensate film forms, with respect to that theoretically predicted. The large deviation between the experimental and theoretical results agrees well with the results of Hassan and Jakob [2] for the condensation on inclined cylinder where the experimental results were found to be 28–100% higher than the analytical results. They attributed this deviation due to the rippling of the condensate film that is not taken into account in the theoretical study.

To avoid the deviation of the theoretical results in predicting the experimental data, a general simi-analytical correlation was deduced to give the Nusselt number in terms of the physical parameters of the condensed vapor, the geometrical parameter of the condensing tube and the orientation of the tube. The semi-analytical correlation is represented as follows

$$Nu = C\left(\frac{h_{fg}\rho_L(\rho_L-\rho_v)g}{k\mu\Delta TL}\right)^{1/4} D(L/D)^n\left(1+\sin^{2.25}\beta\right) \qquad (36)$$

where, the constant (C, n) are (0.985, 0), (0,33, 0.25) and (0.65, 0.791) for vertical, horizontal and inclined tubes, respectively.

The results of semi-analytical correlation (Eqn. (36)) are compared with the experimental and analytical results and represented graphically in Figs. 7 and 8. The comparison between results of semi-analytical correlation and all the experimental results is shown in Fig. 9. Fig. 9 shows that the suggested semi-analytical correlation can predict all the experimental data within ±11%.

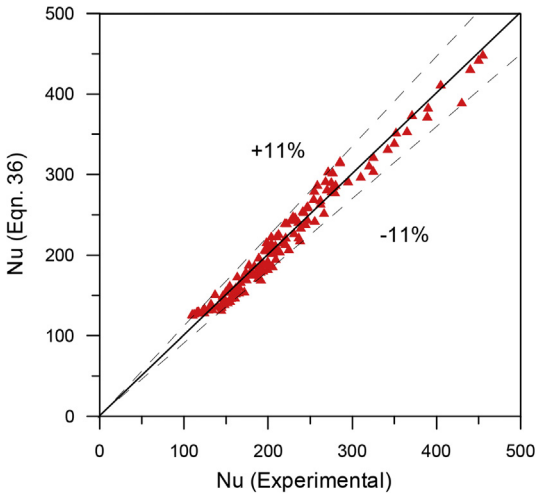

Fig. 9. Comparison between semi-analytical correlation results and experimental results.

5. Summary and conclusions

Comprehensive analytical and experimental investigations for condensation of saturated vapor on smooth tubes with different inclination angles are presented. An analytical model was developed starting from mass, momentum and energy equations to give the condensate film thickness and heat transfer coefficient for any tube orientation in terms of the controlling parameters. In the experimental work, heat transfer due to film-wise condensation of saturated steam on inclined smooth tube has been investigated for tube inclination angles of 0°, 10°, 20°, 30°, 45°, 60° and 90° with the vertical. Variation of average heat transfer coefficient and Nusselt number with the temperature difference and inclination angles obtained from theoretical and experimental work are presented, investigated and compared. Both experimental and theoretical results showed the increase of the Nusselt number with the decrease of the temperature difference and the increase of the tube inclination angle from the vertical. Comparison between the experimental and theoretical results showed fair agreement for vertical and horizontal tubes. However, the deviation increased with tilting the tube from horizontal or vertical position. General semi-analytical correlation was deduced from the experimental data and the theoretical results to accurately predict the Nusselt number during vapor condensation on tubes at different orientations.

References

[1] W. Nusselt, Die Oberflächenkondensation des Wasserdampfes, VDI-Zeitschr. 60 (27) (1916) 541–546 and 60 (28) (1916) 568–578.
[2] K.E. Hassan, M. Jakob, Laminar film condensation of pure saturated vapour on inclined circular cylinder, J. Heat Transf. 80 (1958) 887–894.
[3] H.M.S. Hussein, M.A. Mohamad, A.S. El-Asfouri, Theoretical analysis of laminar-film condensation heat transfer inside inclined wickless heat pipes flat-plate solar collector, Renew. Energy 23 (2001) 525–535.
[4] H.M.S. Hussein, H.H. El-Ghetany, S.A. Nada, Performance of wickless heat pipe flat plate solar collectors having different pipes cross sections geometries and filling ratios, Energy Convers. Manag. 47 (2006) 1539–1549. Elsevier.
[5] J.C.Y. Wang, Y. Ma, Condensation heat transfer inside vertical and inclined thermosyphons, J. Heat Transf. 113 (1991) 777–780.
[6] S. Fiedler, H. Auracher, Experimental and theoretical investigation of reflux condensation in an inclined small diameter tube, Int. J. Heat Mass Transf. 47 (2004) 4031–4043.
[7] M.M. Shah, An improved and extended general correlation for heat transfer during condensation in plain tubes, HVAC&R Res. 15 (5) (2009) 889.

[8] J.P. Meyer, J. Dirker, A.O. Adelaja, Condensation heat transfer in smooth inclined tubes for R134a at different saturation temperatures, Int. J. Heat Mass Transf. 70 (2014) 515–525.
[9] B.-X. Wang, X.-Z. Du, Study on laminar film-wise condensation for vapor flow in an inclined small/mini-diameter tube, Int. J. Heat Mass Transf. 43 (2000) 1859–1868.
[10] S. Lips, J.P. Meyer, Two-phase flow in inclined tubes with specific reference to condensation: a review, Int. J. Multiph. Flow 37 (8) (2011) 845–859.
[11] G. Caruso, D.V. Maio, Heat and mass transfer analogy applied to condensation in the presence of non-condensable gases inside inclined tubes, Int. J. Heat Mass Transf. 68 (2014) 401–414.
[12] G. Caruso, D.V. Maio, A. Naviglio, Film condensation in inclined tubes with noncondensable gases: an experimental study on the local heat transfer coefficient, Int. Commun. Heat Mass Transf. 45 (2013) 1–10.
[13] S.A. Nada, Cooling of very hot vertical tubes by falling liquid film in presence of countercurrent flow of rising gases, Int. J. Therm. Sci. 88 (2015) 228–237.
[14] S.A. Nada, H.F. Elattar, Semi analytical parametric study of rewetting/quenching of hot vertical tube by a falling liquid film in the presence of countercurrent flow of rising vapors, Int. J. Therm. Sci. 99 (2016) 85–95.
[15] G. English, W.T. Jones, R.C. Spillers, V. Orr, Flooding in a vertical upward partial condenser, Chem. Eng. Prog. 59 (1963) 51–53.
[16] S. Fiedler, H. Aurcher, D. Winkelmann, Effect of inclination on flooding and heat transfer during reflux condensation in a small diameter tube, Int. Commun. Heat Mass Transf. 29 (2002) 289–302.
[17] D.G. Thomas, Enhancement of film condensation rate on vertical tubes by longitudinal fins, AICHE 14 (4) (1968) 644–649.
[18] N. Domingo, J.J. Michel, Ammonia condensation on smooth and fluted aluminum tubes, Sol. Energy Eng. Trans. ASME 104 (1982) 9–14.
[19] A.M. Amin, Augmentation of Heat Transfer from Saturated Steam Condensing Around Vertical Tubes (M. Sc. thesis), Cairo University, Egypt, 1990.
[20] G.D. Smith, Numerical Solution of Partial Differential Equation, second ed., Clarendon Press, Oxford, 1978.
[21] C.R. Wylie, L. Barret, Advanced Engineering Mathematics, fifth ed., McGraw-Hill, Japan, 1988.
[22] J.P. Holman, W.J. Gajda, Experimental Method for Engineers, McGraw Hill, New York, 1989.